

Efficient Electrochemical Sensor Based on Multi-Walled Carbon Nanotubes/Gold Nanocomposite for Detection of Dichlorvos Pesticide in Agricultural Food

Yi Chen*, Kuo He, Fengmei Sun, Dong Wei, Hui Li

Key Laboratory of Analysis and Testing of Agricultural Products Food Quality and Safety in Hebei Province, Hebei North University, Zhangjiakou 075000, Hebei, China

*E-mail: yiyi433@sina.com

Received: 25 November 2020 / Accepted: 7 January 2021 / Published: 31 January 2021

This study was conducted to prepare and electrochemically characterize Au@MWCNTs nanocomposite modified GCE (Au@MWCNTs/GCE) as dichlorvos pesticides sensor in agriculture. Structure and morphology studies by SEM and XRD analyses showed the face-centered cubic structure of Au nanoparticles were formed and homogeneously distributed on network-like structure of MWCNTs which indicating to high porosity, large effective surface area and fast electron transfer rate of Au@MWCNTs/GCE. Cyclic voltammetry (CV) and differential pulse voltammetry (DPV) techniques were used to electrochemically characterize Au@MWCNTs/GCE which shows the limit of detection and linear range of dichlorvos sensor were obtained 5 nM and 1-120 μ M, respectively. Comparison of the prepared electrode with other similar reported sensors revealed a low detection limit and reasonable linear range for dichlorvos which is comparable with others carbon and gold nanostructured based sensors due to synergistic effects of Au nanoparticles and MWCNTs. Interference effects, stability and repeatability of dichlorvos sensors were investigated in the presence of different species. Analytical applicability of dichlorvos sensor was studied for prepared real samples of leaf lettuce which indicated acceptable values for recovery in the range of 90.75%-97.50% and relative standard deviation (RSD) in the range of 2.18%-4.85% which indicated Au@MWCNTs/GCE is reliable for the detection of dichlorvos in real samples.

Keywords: Dichlorvos; MWCNTs; Au@MWCNTs nanocomposite; Electrochemical sensor; Real samples

1. INTRODUCTION

Dichlorvos (DDVP; 2, 2-dichlorovinyl dimethyl phosphate) is a commercial organophosphate dominant pesticide employed in domestic insects in the milling and grain handling industries. It effectively harms the insect's DNA and acts on acetylcholinesterase which is related to the insect's nervous system [1]. Thus, it is widely employed to kill bugs, aphids, mosquitoes, caterpillars,

mushroom flies and cockroaches [2]. Furthermore, it shows many side effect on human body such as weakness, headache, dizziness, tightness in chest, wheezing, blurred vision, eye and skin irritation, runny nose, nausea, diarrhea, cyanosis, paralysis, ataxia, convulsions, and cardiac arrhythmias [3, 4]. Furthermore, studies exhibited that organophosphate metabolites lead to attention deficit hyperactivity disorder in children [5, 6].

The high applicants and demands of dichlorvos lead to concerns due to its chronic toxicity and pollution of urban waterways and industrial wastewaters [7, 8]. Accordingly, dichlorvos has been classified as extremely toxic by the World Health Organization (WHO) and banned in European Union (EU). Hence, identification and detection of level of dichlorvos have been important aims of many studies through fluorescence spectra, fluorescence quenching effect, high-performance liquid chromatography, spectrophotometry, mass spectrometry, gas chromatography-mass spectroscopy and electrochemical techniques [9-11].

For several decades, electrochemical sensors and biosensors have been extensively used in determination of pesticide due to their simplicity, fast response and low cost. Modifying the electrode surface in electrochemical sensing systems has promoted sensitivity, stability and accuracy [12-14]. Variety chemical components in composites, doped materials, and various morphology of nanostructures, hybrids and multi-layered films have been revealed improvement in chemical and physical properties and efficiency of sensors [15-22].

Accordingly, this study was carried out for preparation and electrochemical characterizations of Au@MWCNTs/GCE for determination of dichlorvos pesticides in agricultural food.

2. MATERIALS AND METHODS

0.1 g of MWCNTs (99.9 %, Length of 3-5 μm , Zhengzhou Dongyao Nano Materials Co. Ltd., China) was stirred in 6 M nitric acid (68 %, Jinzhou City Jinchangsheng Chemical Co. Ltd., China) for 12 hours to remove the impurities and amorphous carbon and functionalize the negative groups $-\text{COO}^-$ on MWCNTs surface [23]. Then, the resulting suspension was filtered and then washed with deionized water for several times. The functionalized MWCNTs were dispersed in ethanol (95 %, The TNN Development Limited, China) and then ultrasonically added in prepared 0.1 M H_2SO_4 (98 %, Zibo Feiyuan Chemical Co., Ltd., China) solution containing 2 mM $\text{HAuCl}_4 \cdot 2\text{H}_2\text{O}$ (Gold \geq 47.8 %, Shanghai Xinglu Chemical Technology Co., Ltd., China) in volume ratio of 3:1:2.

Prior to the modification of the GCE, the GCE was polished using polishing alumina powder (99%, 2-3 μm , Hangzhou Jiupeng New Material Co. Ltd., China) for 15 minutes and cleaned ultrasonically in ethanol and deionized water for 6 minutes, respectively. Then GCE immersed in a mixture solution of 0.5 M nitric acid and 0.1 M H_2SO_4 in volume ratio of 2:1 for 1 hours and was washed with deionized water. For modification of the cleaned GCE, it was immersed in prepared solution of functionalized MWCNTs and Au sources for 5 hours. After then, the immersed electrode was rinsed by deionized water and immersed again in a prepared solution for 3 hours. Finally, the modified Au@MWCNTs/GCE was rinsed with deionized water and air dried.

The scanning electron microscopy (SEM; Philips 515, Electronics NV, Eindhoven, The Netherlands) and X-ray diffraction (XRD, Haoyuan DX2700 X-ray diffraction with Cu K α radiation ($\lambda = 0.154$ nm), Dandong, China) were employed for characterizations of morphology and crystal structures of prepared electrodes, respectively. CV and DPV analysis were performed on electrochemical system containing potentiostat/galvanostat Methrom Autolab (PGSTAT 30, Eco-Chimie, Utrecht, The Netherlands) in conventional three-electrode electrochemical cell which contained Ag/AgCl(3 M) as reference electrode, Pt wire as counter and the prepared electrode (MWCNTs/GCE and Au@MWCNTs/GCE) as working electrodes. All of electrochemical studies were conducted in 0.1 M phosphate buffer solutions (PBS) as electrolyte in electrochemical cell which prepared of 0.1 M H₃PO₄ (98%, Honghao Chemical Co., Ltd., China) and 0.1 M NaH₂PO₄ (98%, Changzhou Shanglian Chemical Co., Ltd., China) in volume ratio of 1:1. The pH 6.5 of PBS was adjusted with HCl (35%, THE BTTCO OVERSEAS, China) and NaOH (99%, Riotta Botanical Co., Ltd., China) solutions.

The preparation of the real sample was performed using the method which reported in [24]. Four typical green leaf lettuces were separately chopped and pureed in a blender and labeled as S1, S2, S3 and S4. Then, any pureed leaf lettuce was treated with 1 ml of 0.1 M HCl (37 %, Shijiazhuang Xinlongwei Chemical Co., Ltd., China) for 30 minutes and filtered. Then, the 10 ml of filtered mixtures were centrifuged for 10 minutes and then 1 ml of 0.1 M ammonia (28 %, Inner Mongolia Pulisi Chemical Co., Ltd., China) was added in the centrifuged mixtures to adjust the pH to 6.5. The resulting supernatants were diluted with 1 ml PBS and were employed as four prepared real samples for detection of dichlorvos level.

3. RESULTS AND DISCUSSION

SEM images of MWCNTs/GCE and Au@MWCNTs/GCE are shown in Figure 1. The morphology of MWCNTs film in Figure 1a displays a network-like structure which may be favorable for electron transfer [25]. The average diameter of MWCNTs is 65 nm. For Au@MWCNTs nanocomposite in Figure 1b, SEM image shows surface topologies was changed dramatically in present of Au source in preparation solution and many dots are observed which refers to formation and homogeneously distribution of Au nanoparticles on MWCNTs network-like structure. The average diameter of Au nanoparticles on MWCNTs network is 50 nm.

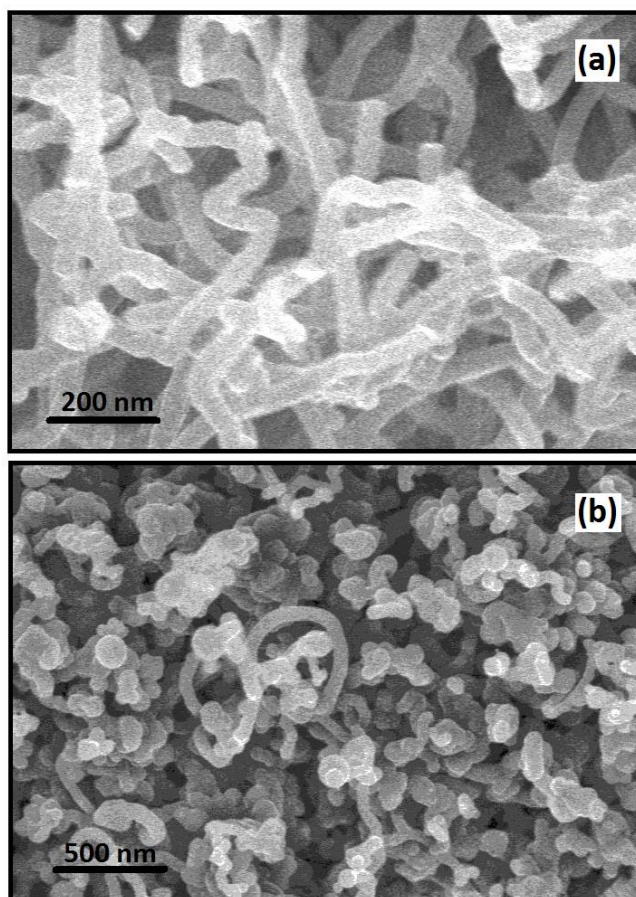


Figure 1. SEM images of (a) MWCNTs and (b) Au@MWCNTs on GCE surface.

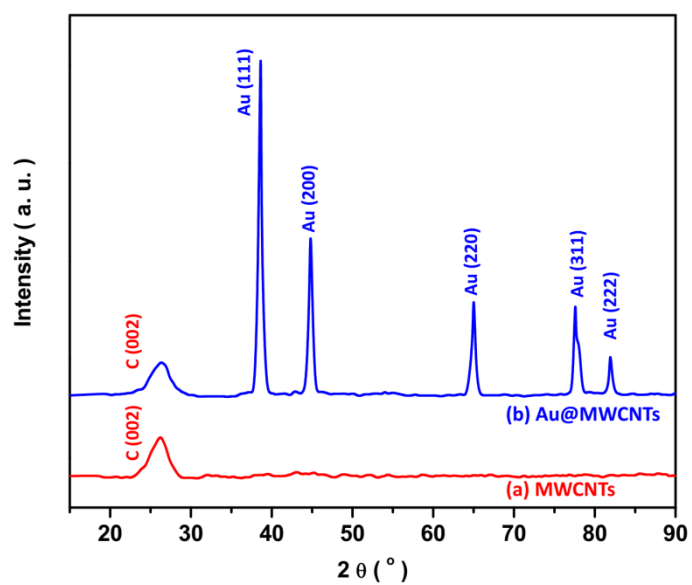


Figure 2. The recorded XRD patterns of (a) MWCNTs and (b) Au@MWCNTs nanocomposite.

Figure 2 displays the recorded XRD patterns of MWCNTs and Au@MWCNTs nanocomposite. The XRD of MWCNTs in Figure 2a shows diffraction peak at 26.12° which refers to typical characteristic (002) plane (JCPDS card No. 26-1077) and the graphitic sidewall of MWCNTs [26]. The XRD of Au@MWCNTs in Figure 2b indicates diffraction peak C (002) which suggests that the anchoring of Au nanoparticles on MWCNTs structure could not demolish the MWCNTs crystal structure. Furthermore, five new peaks are also observed at $2\theta = 38.88^\circ$, 45.05° , 65.21° , 78.11° , and 82.14° which associating to formation of (111), (200), (220), (311), and (222) planes of face-centered cubic structure of Au nanoparticles on MWCNTs (JCPDS card No. 002-1095). Therefore, XRD analysis shows that Au nanoparticles have been strongly anchored on the surface of the MWCNTs.

CVs measurements were performed as electrochemical techniques to study the GCE, MWCNTs/GCE and Au@MWCNTs/GCE in 0.1 M PBS solution pH 6.5 as electrolyte solution in electrochemical cells. Figure 3 shows the initial recorded CVs of the electrodes in potential range from -0.2V to 0.7V at 20mV s^{-1} in presence of $5\ \mu\text{M}$ dichlorvos. As shown, it is not recorded as an observable peak in potential range from -0.2 to 0.7 V for bare GCE. For MWCNTs/GCE, there is a weak anodic peak as electrochemical response for dichlorvos at 0.43 V with current of $1.73\ \mu\text{A}$. Furthermore, the oxidation peak was recorded at 0.31 V with current of $3.57\ \mu\text{A}$ which implies its lower potential and higher current of oxidation peak is observed in comparison to MWCNTs modified GCE. The peak shift to lower potential reveals the electro-catalytic effect towards dichlorvos oxidation, which can be related to formation of oxygen-containing groups on the functionalized MWCNT surface in nitric acid media [27-29]. Furthermore, anchoring of the Au nanoparticles on functionalized MWCNT surface leads to more effective surface area, higher conductivity, and provides the high effective electrostatic interaction for dichlorvos[30-32].

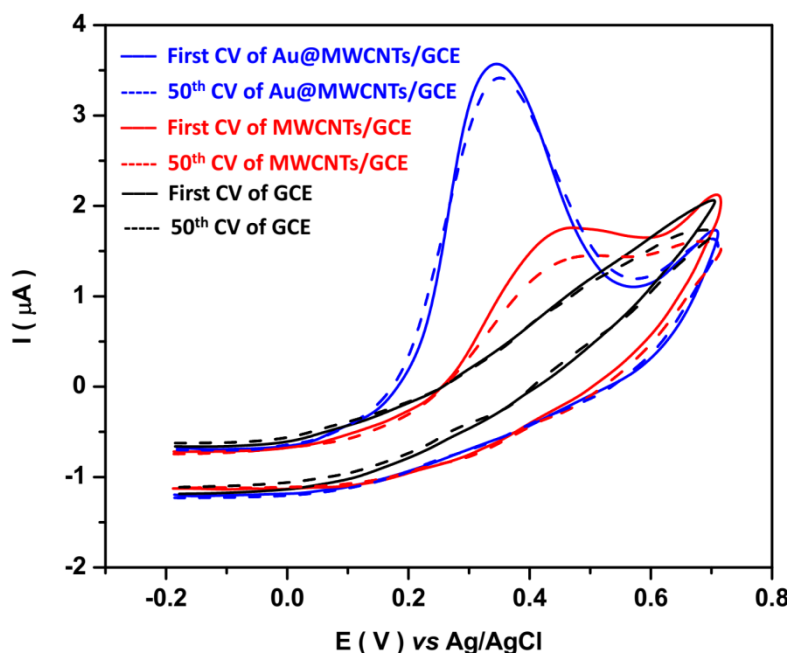


Figure 3. (a) The initial and (b) 50th recorded CVs of GCE, MWCNTs/GCE and Au@MWCNTs/GCE in potential range from -0.2V to 0.7V at 20mV s^{-1} in 0.1 M PBS solution pH 6.5 in presence of $5\ \mu\text{M}$ dichlorvos

Moreover, Figure 3 displays the stability responses of GCE, MWCNTs/GCE and Au@MWCNTs/GCE under record of successive CVs. As observed, the comparison between the initial and 50th recorded CVs of MWCNTs/GCE and Au@MWCNTs/GCE in presence of 5 μM dichlorvos shows 20.0 % and 5.3 % reduction for oxidation peak currents due to adsorption of dichlorvos oxidation product at the electrode surfaces [33, 34]. Furthermore, more stability response of Au@MWCNTs/GCE shows the higher catalytic effect of concurrent Au nanoparticles and functionalized MWCNTs on nanocomposite surfaces [35]. Thus, Au@MWCNTs/GCE was selected for further electrochemical via DPV technique for determination of dichlorvos.

Figure 4a shows the recorded DPV response of Au@MWCNTs/GCE to successive addition 1 μM concentration of dichlorvos in potential range from -0.2V to 0.7V at 20mVs^{-1} in 0.1 M PBS solution pH 6.5. As observed, the oxidation peak current is increased linearly with increasing dichlorvos concentration. The calibration plot in Figure 4b shows a limit of detection of 5 nM for determination of dichlorvos. In order to obtain the linear range value, this study was repeated to successive addition of 20 μM concentration of dichlorvos in electrochemical cells. Figures 5a and 5b show the DPV response and its calibration plot which evidence to the linear range is obtained 1-120 μM .

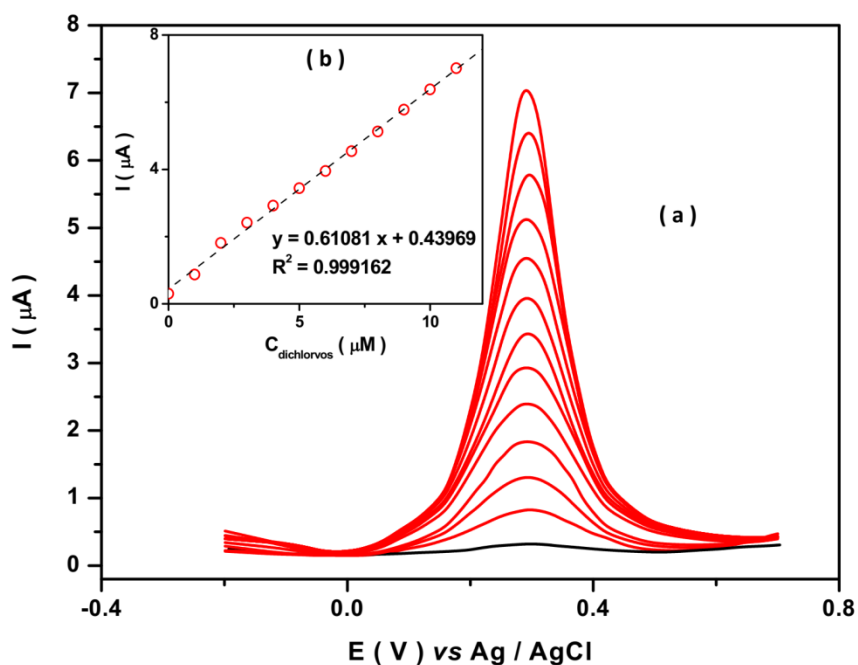


Figure 4. (a) The recorded DPV response of Au@MWCNTs/GCE to successive addition 1 μM concentration of dichlorvos in potential range from -0.2V to 0.7V at 20mVs^{-1} in 0.1 M PBS solution pH 6.5 and (b) its calibration plot.

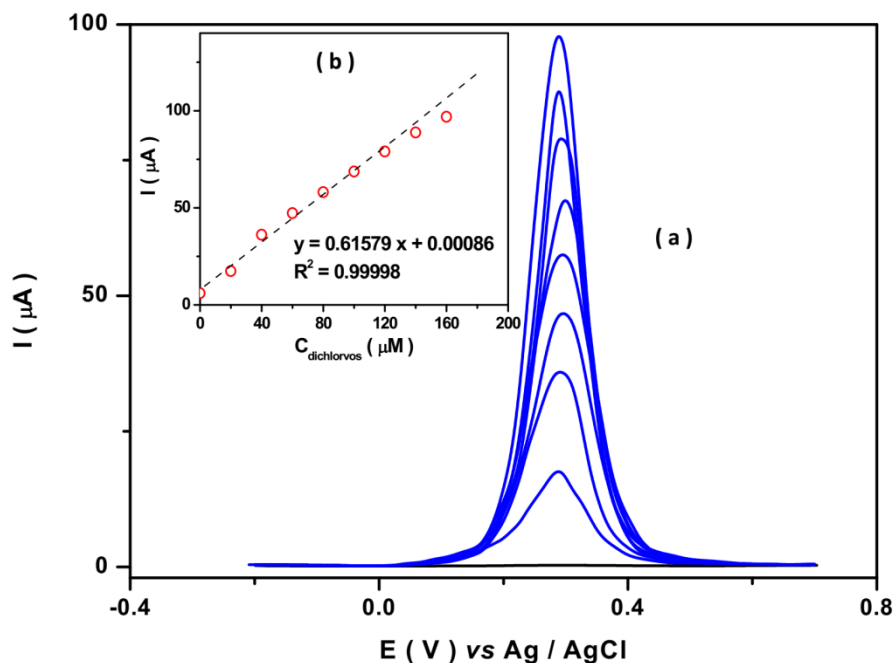


Figure 5. (a) The recorded DPV response of Au@MWCNTs/GCE to successive addition 20 μM concentration of dichlorvos in potential range from -0.2V to 0.7V at 20mVs^{-1} in 0.1 M PBS solution pH 6.5 and (b) its calibration plot.

Table 1. Comparison of Au@MWCNTs/GCE for dichlorvos determination with different reported sensors.

detector	Technique	Detection limit (nM)	Linear range (μM)	ref
Polymerizable luminescence probe	Fluorescence spectra	300	0.5 – 7	[36]
Polymerizable luminescence probe	Spectrophotometry	320	50 – 200	[37]
Carbon dots-Cu(II)	Fluorescence quenching effect	38	0.006 – 0.06	[38]
Molecularly imprinted polymer	High-performance liquid chromatography	0.4	0.002 – 2.262	[39]
Choline oxidase/ Poly(brilliant cresyl blue)/ CNTs modified electrode	Amperometry	1.6	2.5 – 60	[40]
Acetylcholinesterase/rGO@Nafion /GCE	Amperometry	9.05	0.0226 – 0.453	[41]
Acetylcholinesterase/chitosan@TiO ₂ / rGO/ GCE	DPV	29	0.036 – 22.6	[42]
Au nanoparticles/ ferrocene dendrimer/ rGO/ GCE	DPV	210	0.45 – 281.4	[24]
Au@MWCNTs/GCE	DPV	5	1-120	This work

A comparison of the prepared electrode for dichlorvos determination with other similar reported sensors using different techniques is presented in Table 1. It is observed that the preparation of Au@MWCNTs nanocomposite on GCE exhibits a low detection limit and reasonable linear range for dichlorvos which is comparable with others carbon and gold nanostructured based sensors [24, 38, 40-42] due to synergistic effects of Au nanoparticles and MWCNTs.

Interference response of Au@MWCNTs/GCE was investigated for dichlorvos determination using DPV technique in the presence of different species. Table 2 shows the recorded electrocatalytic currents response of Au@MWCNTs/GCE in potential range from -0.2V to 0.7V at 20mVs^{-1} in 0.1 M PBS solution pH 6.5 in successive injections of 2 μM dichlorvos solution and 10 μM of different species containing dichloro-diphenyl-trichloroethane (DDT), benzene-hexachloride (BHC), chloroform, cyanide, benzene, Zn^{2+} , Cu^{2+} , Ni^{2+} , Ca^{2+} , Cd^{2+} , Sb^{3+} , Ag^+ , Hg^{2+} , Fe^{3+} , Pb^{2+} , NH_4^+ , SO_4^{2-} , PO_4^{3-} , CO_3^{2-} , Cl^- , NO_3^- and NO_2^- . As seen, the Au@MWCNTs/GCE presents a considerable electrocatalytic current to injections of dichlorvos solution and injections of other substances do not interfere with the oxidation signal of dichlorvos. These results are similar to reported interfere effect for dichlorvos determination by capillary electrophoresis technique [43, 44], fluorescence quenching effect on carbon dots-Cu(II) system [38] and electrochemical technique on Au nanoparticles/ ferrocene dendrimer/ rGO/GCE [24] and poly(brilliant cresyl blue)/ CNTs modified electrode [40], which the evidence to reasonable selectivity of Au@MWCNTs/GCE. In order to study the repeatability and stability of response of the prepared electrode, the last injection was repeated for 2 μM dichlorvos. The recorded electro-catalytic currents in Table 2 shows the response of electrodes to the last addition of 2 μM dichlorvos is stable and repeatable after introduction of different species in the electrochemical cell.

Table 2. The recorded electro-catalytic currents response of Au@MWCNTs/GCE in potential range from -0.2V to 0.7V at 20mVs^{-1} in 0.1 M PBS solution pH 6.5 in successive injections of 2 μM dichlorvos solution and 10 μM of different species.

Specie	Added (μM)	Electrocatalytic current density ($\mu\text{A}/\text{cm}^2$)	RSD (%)	Specie	Added (μM)	Electrocatalytic current density ($\mu\text{A}/\text{cm}^2$)	RSD (%)
Dichlorvos	2	1.11	± 0.01	Ag^+	10	0.03	± 0.01
DDT	10	0.05	± 0.01	Hg^{2+}	10	0.05	± 0.02
BHC	10	0.04	± 0.02	Fe^{3+}	10	0.05	± 0.02
Chloroform	10	0.05	± 0.01	Pb^{2+}	10	0.07	± 0.03
Cyanide	10	0.07	± 0.03	NH_4^+	10	0.06	± 0.03
Benzene	10	0.04	± 0.02	SO_4^{2-}	10	0.06	± 0.02
Zn^{2+}	10	0.06	± 0.01	PO_4^{3-}	10	0.04	± 0.01
Cu^{2+}	10	0.04	± 0.03	CO_3^{2-}	10	0.02	± 0.01
Ni^{2+}	10	0.04	± 0.01	Cl^-	10	0.05	± 0.02
Ca^{2+}	10	0.06	± 0.03	NO_3^-	10	0.09	± 0.03
Cd^{2+}	10	0.04	± 0.01	NO_2^-	10	0.07	± 0.01
Sb^{3+}	10	0.07	± 0.02	Dichlorvos	2	1.23	± 0.02

Four prepared real samples of leaf lettuce as S1, S2, S3 and S4 applied for study the analytical applicability of the Au@MWCNTs/GCE to determine dichlorvos by standard addition method. Table 3 shows good and acceptable values for recovery in the range of 90.75% – 97.50% and RSD in the range of 2.18% – 4.85% which indicates Au@MWCNTs/GCE is reliable for the detection of dichlorvos in real samples.

Table 3. Analytical applicability of Au@MWCNTs/GCE to determine dichlorvos in real samples.

Sample	Added (μM)	Found (μM)	Recovery (%)	RSD (%)
S1	2.0	1.95	97.50	2.18
S2	4.0	3.63	90.75	3.66
S3	6.0	5.57	92.83	4.78
S4	8.0	7.75	96.87	4.85

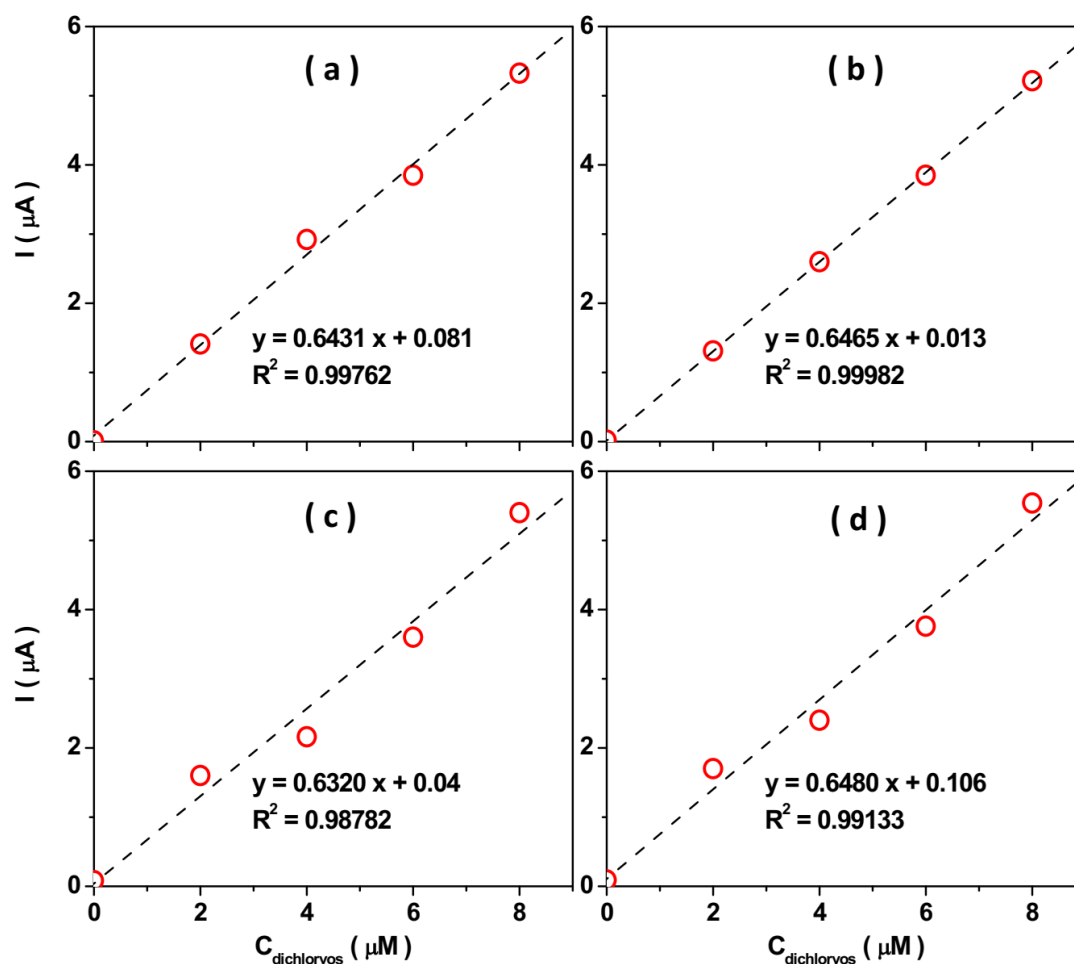


Figure 6. The calibration plots of Au@MWCNTs/GCE for successive addition of 2 μM dichlorvos solution in potential range from -0.2V to 0.7V at 20mVs^{-1} in mixture of 10 ml of 0.1 M PBS and 10 ml of prepared real samples of leaf lettuce (a) S1, (b) S2, (c) S3, and (d) S4.

Furthermore, Au@MWCNTs/GCE was applied to detection the dichlorvos pesticides in four prepared leaf lettuce samples by DPV technique with addition of the 1 μM of dichlorvos solution in electrochemical cell containing 10 ml of 0.1 M PBS and 10 ml of prepared real sample of leaf lettuce solutions pH 6.5 in potential range from 0.2V to 0.7V at 20mVs^{-1} . The calibration plots of samples (S1, S2, S3 and S4) in Figure 6 display the dichlorvos concentrations in electrochemical cells obtained 0.12, 0.02, 0.06 and 0.16 μM for S1, S2, S3 and S4, respectively. Accordingly, the dichlorvos concentrations in real samples are obtained 0.06, 0.01, 0.03 and 0.08 μM for S1, S2, S3 and S4, respectively which suggests the favorable precision and accuracy of prepared electrodes.

4. CONCLUSION

This study was performed to prepare and electrochemically characterize Au@MWCNTs modified GCE for determination of dichlorvos pesticides in agricultural food. Structure characterization by SEM and XRD analyses showed the crystal structure of MWCNTs were modified on GCE in network-like structure. Moreover, formation and homogeneous distribution of Au nanoparticles on MWCNTs were observed for Au@MWCNTs nanocomposite on GCE surface which indicates its higher porosity, larger effective surface area and faster electron transfer rate toward MWCNTs/GCE. CV and DPV techniques were applied to electrochemical studies which shows the lower potential, more sensitive and stable response of Au@MWCNTs/GCE than MWCNTs/GCE for determination of dichlorvos. Limits of detection and linear range of sensor were obtained 5 nM and 1-120 μM , respectively. Comparison of the prepared electrode with other similar reported sensors exhibited a low detection limit and reasonable linear range for dichlorvos which is comparable with others carbon and gold nanostructured based sensors due to synergistic effects of Au nanoparticles and MWCNTs. Interference response and repeatability of dichlorvos sensors were investigated in the presence of different species. Analytical applicability of dichlorvos sensor was studied for prepared real samples of leaf lettuce which displays good and acceptable values for recovery in the range of 90.75%-97.50% and RSD in the range of 2.18%- 4.85% which indicates Au@MWCNTs/GCE is reliable for the determination of dichlorvos in real samples.

References

1. H.U. Okoroiwu and I.A. Iwara, *Interdisciplinary toxicology*, 11(2018)129.
2. R. Gandhi and S.M. Snedeker, *Comments on Toxicology*, 8(2002)85.
3. L. Karalliedde, M. Eddleston and V. Murray, *Organophosphates and health*, (2001)431.
4. H. Karimi-Maleh, Y. Orooji, A. Ayati, S. Qanbari, B. Tanhaei, F. Karimi, M. Alizadeh, J. Rouhi, L. Fu and M. Sillanpää, *Journal of Molecular Liquids*, (2020)115062.
5. M. El-Salam, A. Hegazy, M. Elhady, G. Ibrahim and R. Hussein, *Journal of Environmental and Analytical Toxicology*, 7(2017)2161.
6. J. Rouhi, S. Kakooei, S.M. Sadeghzadeh, O. Rouhi and R. Karimzadeh, *Journal of Solid State Electrochemistry*, 24(2020)1599.

7. M. Miraki, H. Karimi-Maleh, M.A. Taher, S. Cheraghi, F. Karimi, S. Agarwal and V.K. Gupta, *Journal of Molecular Liquids*, 278(2019)672.
8. R. Dalvand, S. Mahmud, J. Rouhi and C.R. Ooi, *Materials Letters*, 146(2015)65.
9. G. Huang, J. Ouyang, W.R. Baeyens, Y. Yang and C. Tao, *Analytica Chimica Acta*, 474(2002)21.
10. F. Tahernejad-Javazmi, M. Shabani-Nooshabadi and H. Karimi-Maleh, *Composites Part B: Engineering*, 172(2019)666.
11. J. Rouhi, S. Mahmud, S. Hutagalung and S. Kakooei, *Micro & Nano Letters*, 7(2012)325.
12. K.E. Toghiani and R.G. Compton, *International Journal of Electrochemical Science*, 5(2010)1246.
13. C. Li, Y. Zhou, X. Zhu, B. Ye and M. Xu, *International Journal of Electrochemical Science*, 13(2018)
14. M. Alimanesh, J. Rouhi and Z. Hassan, *Ceramics International*, 42(2016)5136.
15. R. Hassanzadeh, A. Siabi-Garjan, H. Savaloni and R. Savari, *Materials Research Express*, 6(2019)106429.
16. G. Chen and P. Wang, *International Journal of Electrochemical Science*, 15(2020)2700.
17. H. Savaloni, R. Savari and S. Abbasi, *Current Applied Physics*, 18(2018)869.
18. C. Wang, Q. Song, X. Liu and X. Zhu, *International Journal of Electrochemical Science*, 15(2020)5623.
19. R. Savari, H. Savaloni, S. Abbasi and F. Placido, *Sensors and Actuators B: Chemical*, 266(2018)620.
20. X. Long, C. Deng, G. Xiao, F. Cheng, Y. Zhou, L. Zhao, L. Cai, J. Chen and J. Du, *International Journal of Electrochemical Science*, 15(2020)4964.
21. H. Savaloni and R. Savari, *Materials Chemistry and Physics*, 214(2018)402.
22. Z. Shamsadin-Azad, M.A. Taher, S. Cheraghi and H. Karimi-Maleh, *Journal of Food Measurement and Characterization*, 13(2019)1781.
23. S. Sahebani, S. Zebarjad, J.V. Khaki and A. Lazzeri, *International Nano Letters*, 6(2016)183.
24. L. Yan, X. Yan, H. Li, X. Zhang, M. Wang, S. Fu, G. Zhang, C. Qian, H. Yang and J. Han, *Microchemical Journal*, 157(2020)105016.
25. J. Yu, J. Li, F. Zhao and B. Zeng, *Journal of the Brazilian Chemical Society*, 19(2008)849.
26. M.R. Mohammad, D.S. Ahmed and M.K. Mohammed, *Journal of Sol-Gel Science and Technology*, 90(2019)498.
27. M.V. Naseh, A. Khodadadi, Y. Mortazavi, O.A. Sahraei, F. Pourfayaz and S.M. Sedghi, *World Academy of Science, Engineering and Technology*, 49(2009)177.
28. L. Thi Mai Hoa, *Diamond and Related Materials*, 89(2018)43.
29. N. Naderi, M. Hashim, J. Rouhi and H. Mahmodi, *Materials science in semiconductor processing*, 16(2013)542.
30. P.C. Ma, B.Z. Tang and J.-K. Kim, *Carbon*, 46(2008)1497.
31. I.-H. Cho, D.H. Kim and S. Park, *Biomaterials Research*, 24(2020)1.
32. F. Chahshouri, H. Savaloni, E. Khani and R. Savari, *Journal of Micromechanics and Microengineering*, 30(2020)075001.
33. B.L. Hanssen, S. Siraj and D.K. Wong, *Reviews in Analytical Chemistry*, 35(2016)1.
34. J. Rouhi, S. Kakooei, M.C. Ismail, R. Karimzadeh and M.R. Mahmood, *International Journal of Electrochemical Science*, 12(2017)9933.
35. H.-J. Choi, I.-Y. Jeon, D.W. Chang, D. Yu, L. Dai, L.-S. Tan and J.-B. Baek, *The Journal of Physical Chemistry C*, 115(2011)1746.
36. I.A. Ibrahim, A.M. Abbas and H.M. Darwish, *Luminescence*, 32(2017)1541.
37. H.A. Azab, A.S. Orabi and A.M. Abbas, *Journal of Luminescence*, 167(2015)360.
38. J. Hou, G. Dong, Z. Tian, J. Lu, Q. Wang, S. Ai and M. Wang, *Food Chemistry*, 202(2016)81.
39. Z. Xu, G. Fang and S. Wang, *Food Chemistry*, 119(2010)845.

40. W. da Silva, M.E. Ghica and C.M. Brett, *Sensors and Actuators B: Chemical*, 298(2019)126862.
41. S. Wu, F. Huang, X. Lan, X. Wang, J. Wang and C. Meng, *Sensors and Actuators B: Chemical*, 177(2013)724.
42. H.-F. Cui, W.-W. Wu, M.-M. Li, X. Song, Y. Lv and T.-T. Zhang, *Biosensors and Bioelectronics*, 99(2018)223.
43. Y. Tao, Y. Wang, L. Ye, H. Li and Q. Wang, *Bulletin of environmental contamination and toxicology*, 81(2008)210.
44. R. Mohamed, J. Rouhi, M.F. Malek and A.S. Ismail, *International Journal of Electrochemical Science*, 11(2016)2197.

© 2021 The Authors. Published by ESG (www.electrochemsci.org). This article is an open access article distributed under the terms and conditions of the Creative Commons Attribution license (<http://creativecommons.org/licenses/by/4.0/>).